

# Wound Dressing based on Silver Nanoparticle Embedded Wool Keratin Electrospun Nanofibers Deposited on Cotton Fabric: Preparation, Characterization, Antimicrobial Activity, and Cytocompatibility

Mohammad Mahbubul Hassan,\* Kira Heins, Haotian Zheng

**ABSTRACT:** Wool keratin (WK) protein is attractive for wound dressing and biomedical applications due to its excellent biodegradability, cytocompatibility, and wound-healing properties. In this work, WK-based wound dressings were prepared by depositing WK/polyvinyl alcohol (PVA), and silver nanoparticle (Ag NP)-embedded WK/PVA nanofibrous membranes on cotton fabrics by electrospinning. Ag NPs were biosynthesized by reducing and stabilizing with sodium alginate. The formed Ag NPs were characterized by UV-vis and FTIR spectroscopies and their size was determined by transmission electron microscopy and image analysis. The formed Ag NPs were spherical shaped and had an average diameter of 9.95 nm. The produced Ag NP-embedded WK/PVA nanofibers deposited cotton fabric surface was characterized by FTIR and dynamic contact angle measurements, and the nanofiber morphologies were characterized by scanning electron microscopy. The average diameter of nanofibers formed by 0.1% Ag NP-embedded WK/PVA solution was 146.7 nm. The antibacterial activity of the surface of electrospun nanofibers deposited on cotton fabric was evaluated against the two most common wound-causing pathogens, *Staphylococcus aureus* and *Pseudomonas aeruginosa*. The cotton fabric coated with 0.1% Ag NP-embedded WK/PVA nanofibers showed very good antibacterial activity against both pathogens and MTT assay results showed good cytocompatibility against L-929 mouse fibroblast cells. However, the increase in Ag NP content in the nanofibers to 0.2% negatively affected the cell viability due to the high release rate of Ag ions. The results achieved show that the developed wound dressing has a good potential for wound healing applications.

## 1. INTRODUCTION

The increasing number of patients with chronic wounds caused by diseases, such as diabetes, malignant tumors, infections, and vasculopathy, and also by deep cuts, traumatic injury, and burns has become a major public health challenge, causing severe economic and social burdens. Its prevalence in the general population has been estimated between 1.51 and 2.21 per 1000 population.<sup>1</sup> Over the years, the number of aged populations increased as the life span of individuals increased. According to the World Health Organization (WHO), the number of people aged 80 years or older is expected to triple between 2020 and 2050 to reach 426 million,<sup>2</sup> increasing the load on government health services. Furthermore, the hazards related to human activity, such as increased sports activity, increased injuries for humans resulting in an increasing demand for wound care products, including products used for wound management and prevention of chronic wounds.<sup>3,4</sup> Human skin works as a barrier from pathogens, but cuts or severe injuries create a wound by removing that barrier. Open wounds need to be managed for days to weeks until they are healed or can be closed. Wound care materials are used to debride the wound without damaging healthy tissue, reducing infection and complication, and facilitating the healing process.

The skin is the largest organ of the human body, which is composed of two distinct layers, the dermis, and epidermis. The outermost epidermis layer is composed of layers of differentiated keratinocytes, which function as a barrier to protect the body against the environment.<sup>5</sup> A wound is an

injury or tear in the skin surface due to physical, chemical, mechanical, or thermal damage. The cut or injury to the skin causes the loss of the barrier function of the organ, dehydration, bacterial invasion, or even death.<sup>6,7</sup> Bacterial infection is one factor that has a significant effect on the wound-healing process. Infections can slow down the healing process and lead to chronic wounds.<sup>8</sup> *Staphylococcus aureus* and *Pseudomonas aeruginosa* are the common bacteria detected in more than 70 % of the wounds.<sup>9,10</sup> The basic function of a wound dressing is to cover the wound and prevent it from contamination with bacteria. The choice of the right dressing depends on depth, shape, and size, the amount of wound exudates, the location of the wound, and also the health and age of the patient.

Modern wound dressings have several layers. The construction of typical wound dressings is shown by a schematic diagram in Figure 1. The top layer is a hydrophobic tape that has adhesive on the inner surface so that the bandage can stick to the human skin surface and the wound dressing does not dislodge during its use. The mid layer is made of one or two layers of moisture-absorbent cotton gauze fabric which provides dimensional stability and strength to the bandage and eases the removal of the bandage after its use. The bottom layer which is in contact with the wound is generally made of polyurethane foam (PUF), which is porous and highly moisture adsorbent allowing absorption of wound exudates slowly healing the wound. A few dressings like hydrocolloids, alginate acids, and hydrogels, along with supporting textile materials, are now available in the market. Traditional wound dressing products

including cotton gauze, plasters, and bandages are used as primary or secondary dressings for protecting the wound from dirt and bacteria. A range of wound dressings in the form of films, foams, hydrogels, and hydrocolloids, supported on textile materials are now available in the market.<sup>11,12</sup> They act as a barrier against bacteria and other contaminants. Nylon-derived semi-permeable film dressings, such as Opsite®, Tegaderm®, etc., are mainly recommended for superficial wounds, but they have limited absorption capacity and cause maceration of the wound and the healthy tissues surrounding it.<sup>13</sup> A few dressings like hydrocolloids, alginates, and hydrogels, along with supporting textile materials, are also available. Hydrogel dressings made of synthetic polymers, such as Intrasite®, Nu-gel®, and Aquaform®, are used for dry chronic wounds, ulcers, and burn wounds but they have poor mechanical strength and are not biocompatible.<sup>14</sup> Alginate wound dressings, such as Kaltostat®, and Algisite®, accelerate the healing process.<sup>15</sup> These wound dressings only heal the wound by removing the exudates and giving protection from outside environments, but they cannot prevent bacterial infections. Bioactive wound dressings made of collagen, chitosan, and hyaluronic acid are non-toxic, and biodegradable, and encourage natural healing of wounds.<sup>16–18</sup> Recently, antibacterial wound dressings containing ionic silver or iodine as an antibacterial agent, such as ComfortFoam® Ag, Iodofoam®, Tegaderm® Ag, ALGICELL® Ag, and Kerracel® Ag, have come to the market, but they are only effective against selective pathogens.<sup>19</sup> Moreover, prolonged use of iodine leads to skin irritation and staining.<sup>20</sup> The release of iodine or silver ions from them into wounds cannot be sustained.

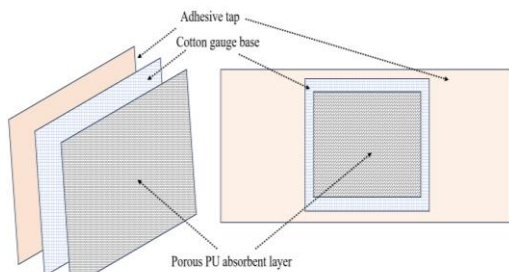


**Figure 1.** Schematic diagram of ordinary wound dressings or bandages.

Keratin is a polyamino acid-based natural protein polymer, which can be extracted from wool fibers, animal hairs, animal horns, nails, and other parts of animals. As a protein polymer, keratin is highly biocompatible and biodegradable. Recently, WK has been extensively studied as foam, film, powder, nanofibrous mat, fiber, and hydrogel for wound healing.<sup>21–23</sup> A hydrogel made from human hair keratin mixed with a natural flavonoid and psyllium gelling agent,<sup>24</sup> and wool keratin (WK)/hydrocalcite,<sup>25</sup> have been investigated as wound dressings. However, as a protein, WK may promote bacterial growth as it is not an antimicrobial agent. These wound dressings only heal the wound by removing the exudates and giving protection from surrounding environments but prevent bacterial infections. Therefore, there

is a need to develop a bioactive wound dressing that not only removes exudates but also releases antibiotics to facilitate quick healing of wounds by killing bacteria.

Electrospun nanofibrous mats of biodegradable protein polymers are widely studied for wound healing because of their high fiber surface, biocompatibility, biodegradability, and fibroblast cell viability area that allows cell binding, such as composites of electrospun gelatine/human hair keratin,<sup>26</sup> cellulose/pectin/soy protein/pomegranate peel extract,<sup>27</sup> keratin/VEGF-incorporated honey,<sup>28</sup> and polyvinyl alcohol (PVA)/graphene oxide, and ZnO-incorporated silk fibroin,<sup>29</sup> etc. Thymol,<sup>29</sup> curcumin,<sup>30</sup> and Ag nanoparticles,<sup>31</sup> have been extensively studied as an antibiotic agent to provide antibacterial activity to the electrospun nanofibrous membranes. Electrospun Ag NP-embedded biopolymeric nanofibrous mats have been studied as wound dressings. Mahmoudi et al. studied electrospun Ag NP-embedded PVA/bioactive glass nanomat as a wound dressing, which exhibited  $93.6 \pm 1.4$  % cell viability along with strong antibacterial activity against *Staphylococcus aureus* and *Escherichia coli*.<sup>32</sup> Electrospun nanomat of Ag-Fe nanoparticle embedded polycaprolactone showed minimal cellular toxicity and considerable antimicrobial properties against some drug-resistant pathogens.<sup>33</sup> Ag NP-embedded polyurethane/human hair keratin electrospun nanomats were also studied as wound dressings.<sup>34</sup> Electrospun nanofibrous wound dressing of keratin extracted from wool fibers, hairs, and feathers has been studied for wound healing. Several articles reported the Ag ion release characteristics of Ag NP containing nanofibrous membranes,<sup>35,36</sup> but no article reported the Ag ions release characteristics of Ag NP containing keratin/PVA nanofibrous membrane deposited on cotton fabrics. Wool keratin has an advantage over other natural polymers as it is a natural protein polymer with excellent cytocompatibility. Wool keratin studied by others is mostly hydrolyzed keratin.

In this work, we used S-sulfonated high molecular weight wool keratin containing Bunte-salt groups extracted from New Zealand merino wool fibers to prepare a bi-layered wound dressing by depositing Ag NP-embedded keratin/PVA nanofibers on cotton fabric. The Ag nanoparticles were synthesized by reducing and stabilizing with brown algae-derived sodium alginate (NA). The antibacterial activity was evaluated against two common pathogens available in most wounds and cell viability and cell proliferation were assessed against L-929 mouse fibroblast cells. This work, for the first time, is reporting the antibacterial and cell viability of Ag nanoparticle embedded wool keratin (AgNP-WK)/PVA nanofiber-deposited-cotton wound dressing as well as the release of Ag ions from them over 7 days.

## 2. RESULTS AND DISCUSSION

### 2.1. Color, Shape, and Size of NA-stabilized Ag NPs.

The characterization of Ag NPs was conducted to confirm the successful conversion of AgNO<sub>3</sub> to Ag NP by NA and to determine the size, shape, and characteristics of the formed Ag NPs. The small spherical Ag NPs usually show a surface plasmon resonance band between 350 and 500 nm with a peak position at 390 to 430 nm.<sup>37</sup> The UV-visible spectrum

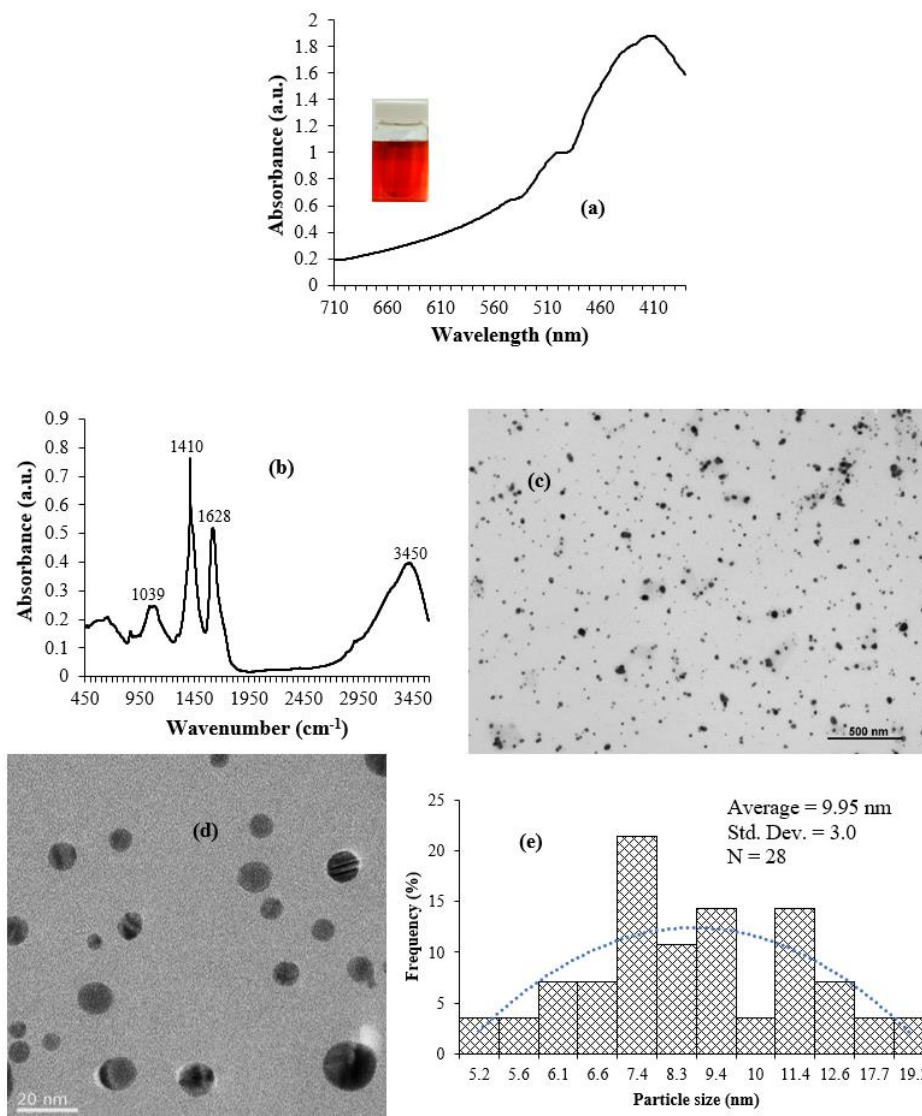


**Figure 2.** UV-vis (a) and FTIR (b) spectra, and TEM image (c, d) and particle size distribution (e) of NA-stabilized Ag NPs.

of an aqueous dispersion of NA-stabilized Ag NPs is shown in Figure 2(a). The spectrum of Ag NPs showed a narrow surface plasmon band at 415 nm, confirming the synthesis of Ag NPs and suggesting the polydispersity and nanocrystalline character of the formed nanoparticles. The analysis of UV-vis spectra suggests that the formed nanoparticles have a diameter of 10 to 20 nm,<sup>37</sup> which is consistent with the size of nanoparticles measured by TEM, which we discussed below. The color of the Ag NPs dispersion also turned to golden yellow, which was highly stable, further suggesting surface plasmon resonance phenomena induced by the Ag NPs and their stabilization with NA due to the ionic interaction between carboxyl groups and Ag NPs.

Figure 2(b) shows the FTIR spectrum of Ag nanoparticles reduced by NA. The spectrum shows IR bands at 1039, 1410, 1628 and 3450  $\text{cm}^{-1}$ . The broad peak at 3450  $\text{cm}^{-1}$  could be associated with the hydroxyl groups of Ag nanoparticles and NA. Alginate usually shows an IR band at 1640  $\text{cm}^{-1}$  due to the C–O stretching of the –COOH groups, but the NA-stabilized Ag NPs showed an IR band at 1628  $\text{cm}^{-1}$

shifted from 1640  $\text{cm}^{-1}$  suggesting interaction between carboxyl groups of NA and hydroxyl groups of Ag NPs. The IR band at 1039  $\text{cm}^{-1}$  can be associated with the C–H stretching vibrations of NA. The spectral analysis suggests the presence of NA in Ag NPs, which stabilized them. The electrostatic attraction between anionic carboxyl groups of alginate and the cationic Ag NPs provided Ag NPs with long-term stabilization.

To observe the morphology of the formed Ag NPs, a TEM image was recorded. Figs. 2(c) to 2(e) show the TEM images and the corresponding particle size distribution of Ag NPs formed by the reduction of  $\text{AgNO}_3$  by NA. The TEM images confirmed the formation of spherical Ag NPs that exhibited polydispersity. The nanoparticles formed no agglomeration suggesting excellent stabilization by NA. The statistical size distributions of Ag NPs presented in Figure 2(e) exhibit a narrow size distribution, which has a range of 5.2 to 19.6 nm with an average size of  $\sim 10$  nm, which is consistent with their UV-vis spectrum and in agreement with results achieved by others.<sup>38</sup>

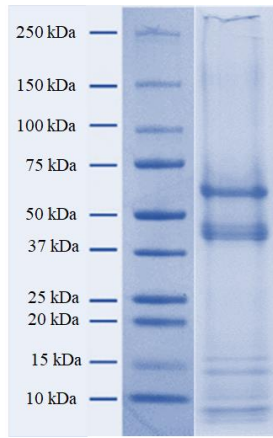


**Figure 3.** SDS-PAGE electrophoresis analysis results of keratin extracted from New Zealand merino wool fibers.

**2.2. Molecular Weight Distribution of Extracted Keratin.** SDS-PAGE analysis of keratin protein extracted from New Zealand merino wool fiber was conducted to assess the molecular weight distribution of various types of proteins. The extracted keratin had mainly two types of protein, intermediate filament proteins (IFPs) and keratin-associated proteins (KAPs). In Figure 3, the IFP Type II proteins appear as a strong band just above the 50 kDa protein marker (the structural  $\alpha$ -keratins), and IFP Type I proteins as three weaker bands between 37 and 50 kDa protein marker.<sup>39,40</sup> On the other hand, the major KAPs are concentrated between 10 and 15 kDa protein markers, the fractions rich in glycine and tyrosine content, while the opaque contributions between 15 and 25 kDa indicate the so-called 'high sulfur' matrix protein, the  $\gamma$ -keratins.<sup>41</sup> The results obtained are consistent with published results.<sup>40,41</sup>

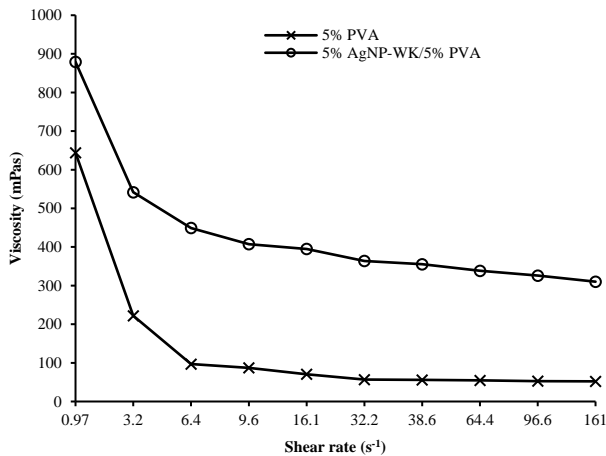


**Figure 4.** Effect of shear rate on the viscosity of 5% PVA solution and 5% PVA + 5% AgNP-WK solution at 22 °C.

**2.3. Rheology of PVA and AgNP-WK-PVA Solutions Used for Electrospinning.** The measurement of the rheology of polymer solution is important to assess their bead-free electro-spinnability. The 10% Ag NP-WK/PVA

solutions containing 0.1 and 0.2% Ag NPs are denoted as 1AgNP-WK-PVA and 2AgNP-WK-PVA respectively. In this work, 5% neat PVA solution produced almost bead-free, and 5% AgNP-WK + 5% PVA solution provided bead-free nanofibers by electrospinning, and therefore their rheological characteristics were assessed. Figure 4 shows the effect of shear rate on the viscosity of 5% PVA, and 5% AgNP-WK + 5% PVA solution at room temperature (22 °C). The addition of AgNP-WK to PVA considerably increased the viscosity of neat PVA due to considerable hydrogen bonding between the hydroxyl groups of PVA and the amino and carboxyl groups of WK protein. The viscosity of the polymer solution was adjusted to ensure the production of bead-free nanofibers. The results suggest that a viscosity of  $\sim$ 900 mPa is required to prepare bead-free nanofibers from a mixed solution of WK/PVA.

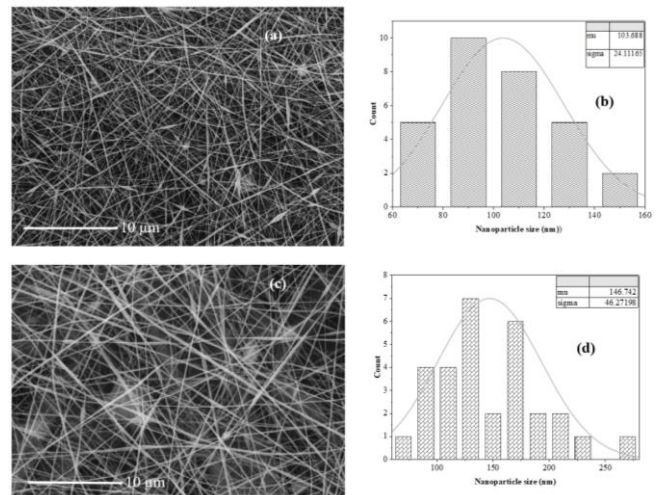


**Figure 5.** SEM images and diameter distribution of cotton fabric coated with PVA (a, b) and (c, d) 1AgNP-WK-PVA nanofibrous membranes.

**2.4. Characterization of the AgNP-WK/PVA Nanofiber-deposited Cotton Fabric.** **2.4.1. Morphological Characteristics.** The surface morphologies and diameter of neat PVA and 1AgNP-WK-PVA nanofibers were analyzed using SEM. Representative SEM micrographs and fiber diameter distribution of pristine PVA and 1AgNP-WK-PVA nanofibers are shown in Figure 5. In both cases, the produced nanofibers are uniformly sized, but few beads were formed, especially in the case of neat PVA. The formed nanofibers are quite randomly oriented across the produced nanofibrous mats exhibiting a uniform distribution without any noticeable bead formation except for neat PVA which formed few beads. The nanofibers produced from a neat PVA had an average diameter of  $\sim$ 103.6 nm but in the case of 1AgNP-WK-PVA, the diameter of nanofibers considerably increased ( $\sim$ 146.7 nm). The addition of AgNP-WK to PVA led to an increase in viscosity, hence increasing fiber diameter. It is known that in electrospinning, the increase in viscosity of the polymer solution or the increase in polymer concentration increases the diameter of the produced nanofibers.<sup>42</sup> The examination of the morphological structure of

nanofibers produced from a mixed solution of AgNP-WK and PVA showed no noticeable phase separation between WK and PVA, showing good compatibility between the two polymer phases.

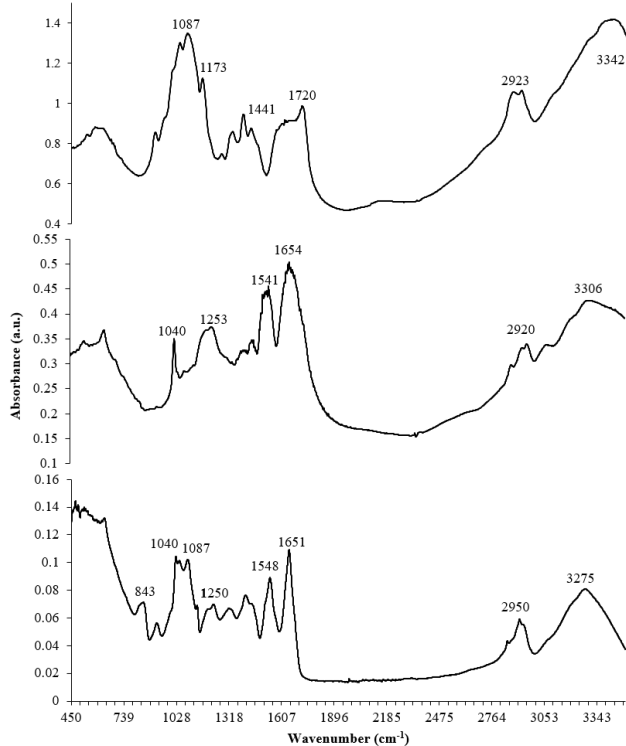


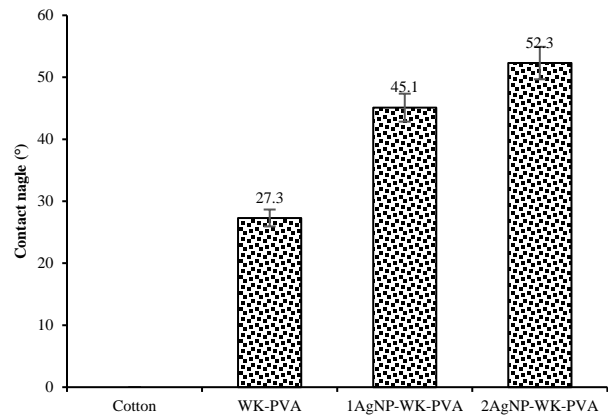
**Figure 6.** ATR-FTIR spectra of neat PVA (top), neat WK (middle), and 1AgNP-WK-PVA (bottom) nanofibers.

**2.4.2. Chemical Characterization.** FTIR spectral analysis was conducted to evaluate the interaction between PVA, WK, and Na-stabilized Ag NPs in the electrospun nanofibers deposited on cotton fabrics. Figure 6 shows the FTIR spectra of PVA and AgNP-WK-PVA nanofibers deposited on cotton fabric. The FTIR spectra of neat PVA, AgNP-WK/PVA nanofibers deposited on a cotton fabric. The spectrum of PVA shows major IR bands at 823, 1087, 1173, 1441, 1720, 2923 and 3342  $\text{cm}^{-1}$ . Of them, IR bands at 3342 and 2923  $\text{cm}^{-1}$  are associated with hydroxyl groups and stretching vibrations of C-H from alkyl groups of PVA. The IR bands at 1720, 1441, 1173, and 1087  $\text{cm}^{-1}$  can be attributed to the ester (C=O),  $\text{CH}_2$ , C-O, and C-O-C groups of PVA respectively.<sup>43</sup> The presence of an ester-related IR band confirms the presence of vinyl acetate groups, which is indicative of the non-hydrolyzed poly (vinyl acetate) group present in the PVA. The IR band of neat WK shows typical keratin-related IR bands at 1654, 1541, and 1253 that could be attributed to amide (I), amide (II), and amide (III) respectively.<sup>44</sup> The sharp IR band at 1040 could be attributed to the Bunte salt groups formed by the breaking of the disulfide linkage of WK and oxidation.<sup>45</sup> The IR band observed at 2923  $\text{cm}^{-1}$  is associated with the stretching vibration of the  $-\text{CH}_2$  group. In the case of the IR spectrum of AgNP-WK/PVA nanofibers, similar IR bands of PVA and WK are present, but

their position slightly changed (especially the IR bands of amides and hydroxyl groups moved downwards of wavenumber) suggesting the interactions between functional groups of WK and PVA, such as hydrogen bond formation.

Figure S2 (Supporting Information) shows the interactions between AgNP-WK and PVA by a schematic diagram. PVA has many hydroxyl groups, but WK has amino ( $-\text{NH}_2$ ), carboxyl ( $-\text{COOH}$ ), and hydroxyl ( $-\text{OH}$ ) groups. The amino, carboxyl, and hydroxyl groups of keratin protein form hydrogen bonds with the hydroxyl groups of PVA, which provided stability and decreased the water-solubility of the formed AgNP-WK-PVA nanofibers.

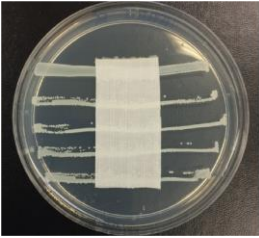
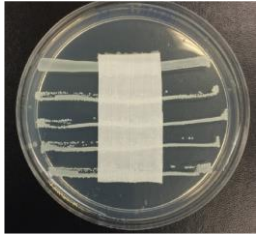
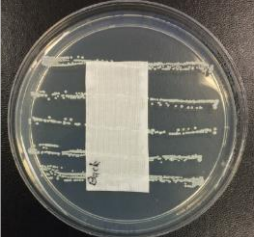
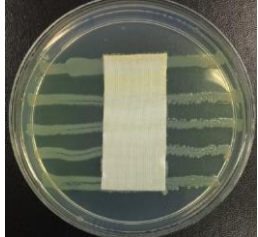
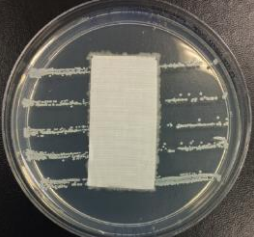
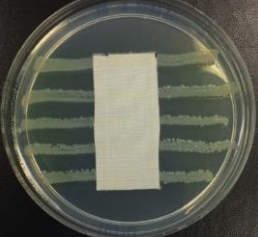
**2.4.3. Contact Angle.** The deposition of Ag nanoparticles on the fiber surface considerably increases its hydrophobicity but the wound dressing surface in contact with the wound needs to have high hydrophilicity. Therefore, the contact angle measurement of AgNP-WK/PVA nanofibers deposited on cotton fabric surface was conducted whether it changed the hydrophilicity of its deposited surface. Figure 7 shows the contact angle of surfaces of uncoated and AgNP-WK/PVA nanofibers deposited on cotton fabrics. The cotton fabric used in this work is highly hydrophilic and the contact angle was 0 as the water droplet placed on the fabric immediately vanished and soaked by the fabric. The nanofiber-coated cotton fabric also showed similar behavior suggesting that the deposition of AgNP-WK/PVA nanofibers on cotton fabric did not at all change its hydrophilicity as PVA and WK both are hydrophilic. The incorporation of Ag NPs only marginally changed the contact angle of WK-PVA-deposited cotton fabric and still, was highly hydrophilic.



**Figure 7.** The contact angle of surfaces of untreated cotton fabric and cotton fabric coated with WK-PVA, 1AgNP-WK-PVA, and 2AgNP-WK-PVA nanofibers.

**2.5. Antibacterial Activity.** Antimicrobial wound dressings have advantages over ordinary wound dressings as they protect wounds against bacterial infection, a common occurrence for various wounds. As Ag NPs are known to provide strong antibacterial protection against a wide range of bacteria, the antibacterial activity of WK/PVA and AgNP-WK/PVA nanofiber-deposited-cotton fabric was evaluated to see their potential bioactivity against two classes of bacteria commonly available in various wounds. Table 1 shows

**Table 1. Antibacterial activity of uncoated and various coated cotton fabrics against *Staphylococcus aureus* and *Pseudomonas aeruginosa*.**

Sample ID.	Antibacterial activity against	
	<i>Staphylococcus aureus</i>	<i>Pseudomonas aeruginosa</i>
Control cotton fabric	No zone of inhibition. Strong growth directly under the fabric	No zone of inhibition. Strong growth directly under the fabric
		
WK-PVA nanofibers on cotton fabric	No zone of inhibition. Weak growth directly under the fabric	No zone of inhibition. Weak growth directly under the fabric
		
1AgNP-WK-PVA nanofibers on cotton fabric	No zone of inhibition. No growth directly under the fabric	No zone of inhibition. No growth directly under the fabric
		
2AgNP-WK-PVA nanofibers on cotton fabric	No zone of inhibition. No growth directly under the fabric	No zone of inhibition. No growth directly under the fabric
		

the antibacterial performance of uncoated cotton fabrics and cotton fabrics coated with WK/PVA and AgNP-WK/PVA nanofibers against *Staphylococcus aureus* and *Pseudomonas aeruginosa*. The uncoated cotton fabric did not show any antibacterial activity against both types of bacteria as strong growth of bacteria was observed under the tested surface and also over the fabric. The surface of cotton fabric coated with WK/PVA nanofibers provided some levels of hindrance against bacterial growth due to the presence of WK as amino groups of WK can interact with bacterial cells. The uncoated and AgNP-WK/PVA nanofiber-coated fabrics did

not show any zone of inhibition. Tran et al. found that the addition of WK to cellulose provided some level of antibacterial activity against *Staphylococcus aureus* and *Escherichia coli*.<sup>46</sup> It is also known that polypeptides are potent antibacterial agents that are effective against a wide range of Gram-positive and Gram-negative bacteria.<sup>47</sup> On the other hand, cotton fabric surface coated with 1AgNP-WK-PVA and 2AgNP-WK-PVA nanofibers also did not show any zone of bacterial inhibition indication of limited leaching of Ag NPs from the AgNP-WK/PVA nanofibers. We used quite a low dosage of Ag NPs, 0.1 and 0.2% on the weight of the

combined weight of keratin and PVA causing a very low release of Ag ions. The degradation of WK-PVA nanofibers was slow as keratin was insoluble under the testing conditions providing no zone of inhibition. However, both samples showed adequate antibacterial activity as no bacterial growth was observed under the tested samples for both types of bacteria.

Capping agents are used to modify the surfaces of silver nanoparticles, which can change their dissolution behavior and release Ag ions responsible for killing bacteria. The released Ag<sup>+</sup> ions penetrate bacterial cells and can inhibit the growth of bacteria or exert toxicity by damaging the cellular membrane.<sup>48</sup> The WK has an isoelectric point of 4.7, i.e., keratin is cationic below pH 4.7 and anionic above that pH.<sup>49</sup> In our case, no zone of inhibition was observed for the cotton fabric coated with AgNP-WK/PVA nanofibers possibly because of the combined effect of anionic keratin and NA the Ag ions released from the Ag NPs contained in the nanofibers and therefore supposed to provide long term antibacterial activity.

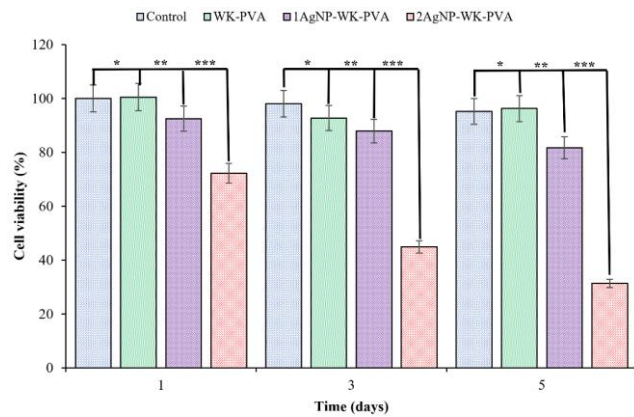


**Figure 8.** In vitro cell viability of L-929 fibroblast cells on WK-PVA, 1AgNP-WK-PVA, and 2AgNP-WK-PVA nanofibers deposited on cotton fabrics. L-929 cells were incubated on cotton bandages containing 0, 0.1, and 0.2% Ag NPs for 1, 3, and 5 days, and cell viability was measured using the MTS assay (P value >0.05).

**2.6. Cell viability by MTT Bioassay and Cell Proliferation.** The MTT assay and CCK-8 assay were conducted to determine the fibroblast cell viability against the prepared WK-PVA and AgNP-WK-PVA nanofiber. Cell viability higher than 75% is considered as noncytotoxic.<sup>50</sup> Figure 8 shows the viability of L-929 fibroblast cells in the presence of no nanofibers (control), and also L-929 fibroblast cells seeded on nanofibrous WK-PVA, 1AgNP-WK-PVA and 2AgNP-WK-PVA nanofibers deposited on cotton fabrics for 1-, 3-, and 5-days period and the proliferation rate and cell viability were determined using the MTT assay. The control showed excellent cell viability over a 5-day study period. In the case of cotton fabric coated with WK-PVA nanofibers, cell growth at day 1 was 92.7%, which gradually increased to 100.5% over the 5 days. However, the cotton fabric coated with 1AgNP-WK-PVA nanofibers showed a decrease in cell growth over 5 days, which is consistent with published

results.<sup>51</sup> On day 1, the L-929 fibroblast cell growth was 92.5%, which decreased to 81.6% after 5 days of incubation. The cell growth considerably decreased when the Ag content of the WK-PVA nanofibrous membrane deposited on cotton fabric was increased to 2% (i.e., 2AgNP-WK-PVA). For this sample, the cell growth on day 1 was 72.2%, which decreased to 31.3% on day 5. Overall, cotton fabric coated with 2AgNP-WK-PVA exhibited the best results in terms of antibacterial activity but low cytocompatibility.

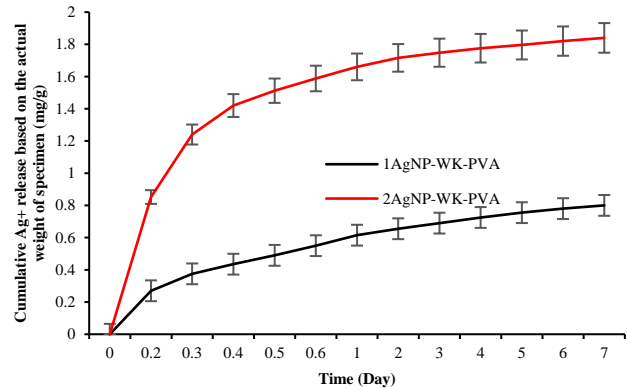


**Fig. 9.** Cumulative release profiles of Ag<sup>+</sup> ions from 4 h glutaraldehyde crosslinked 1AgNP-WK-PVA and 2AgNP-WK-PVA-coated cotton fabric samples.

**2.7. Release of Ag ions from the 1AgNP-WK-PVA and 2AgNP-WK-PVA-coated cotton fabrics.** To identify the cause of considerably lower cell viability and cell proliferation exhibited by the cotton fabric coated with 2AgNP-WK-PVA, we studied the Ag ion release profile of cotton fabrics coated with 1AgNP-WK-PVA and 2AgNP-WK-PVA nanofibrous membranes. The mixed solutions of 1AgNP-WK-PVA and 2AgNP-WK-PVA contained 0.1 and 0.2% Ag NPs respectively, it was calculated that the membranes contained a maximum of 2 and 5 mg/g Ag respectively. Fig 9 shows the cumulative Ag ions release profile of cotton fabrics coated with 1AgNP-WK-PVA and 2AgNP-WK-PVA nanofibrous membranes in phosphate buffer saline at pH ~7.4, and 37°C (which is the normal human body temperature). It can be seen that in the case of cotton fabric coated with 1AgNP-WK-PVA, the release rate was quite slow, and the maximum release was achieved after 7 days, which was ~80% of its Ag loading. On the other hand, the cotton fabric coated with 2AgNP-WK-PVA showed quite high Ag, and most of the Ag was released within the first day of the test. The Ag ions released from this treated fabric are almost 92% of the total Ag loading of these samples. The low cell viability exhibited by the cotton fabric coated with 2AgNP-WK-PVA nanofibrous membrane was due to considerably higher Ag ions release from the test sample causing the death of cells and exhibiting poor cell viability. The release profile suggests that the cotton fabric coated with 1AgNP-WK-PVA nanofibrous membrane offers better sustained release compared to the cotton fabric coated with 2AgNP-WK-PVA nanofibrous membrane. Kim

## 4. EXPERIMENTAL SECTION

**3.1. Materials.** Scoured and bleached cotton fabric of 110 g/m<sup>2</sup> was procured from a local textile manufacturing company. The fabric was autoclaved to kill any microbes present in it. The high molecular weight S-sulfonated keratin protein used in this work was extracted from New Zealand merino wool fibers by oxidative sulfitolysis, which was supplied by Keraplast Limited (New Zealand). Poly(vinyl alcohol) or PVA (average molecular weight of 80,000, and 90% hydrolyzed), silver nitrate (AgNO<sub>3</sub>), NA, acetic acid, dithiothreitol (DTT), Coomassie Brilliant Blue R-250 dye, fetal bovine serum (FBS), phosphate buffer saline, penicillin, and streptomycin were of analytical reagent grade and were purchased from Sigma-Aldrich Chemicals (USA). The Mueller Hinton agar and Trypticase Soy Broth were purchased from Merck (Germany) and Gibco (Germany) respectively. The Dulbecco's modified eagle medium (DMEM), CyQUANT™ MTT cell viability assay kit, and L-929 mouse fibroblast cell line used for the assessment of cell proliferation and cell viability were purchased from Thermo Fisher Scientific Corporation (USA). The LDS sample loading buffer (4X) containing lithium dodecyl sulfate and NuPAGE MOPS SDS running buffer was purchased from Invitrogen Corporation (Waltham, USA). The bacterial cultures of *Staphylococcus aureus* (ATCC 6538) and *Pseudomonas aeruginosa* (ATCC 25619) were purchased from Environmental Science Research Limited (Porirua, New Zealand).

**3.2. Synthesis of Ag Nanoparticles.** NA-reduced and stabilized Ag NPs were prepared by AgNO<sub>3</sub> as a source of Ag and NA as a reductant for Ag and stabilizer for the formed Ag NPs. To prepare Ag NP dispersion, 50 ml of 1000 ppm aqueous solution of AgNO<sub>3</sub> was taken to a three-neck glass bottle fitted with a condenser and covered with aluminum foil to protect from light. 50 mL of 4 g/L aqueous solution of NA was added to it with vigorous continuous stirring at a mass ratio of Ag to NA of 1:10. The mixture was then heated at 70 °C for 2 h with continuous stirring. The color of the solution turned to reddish-brown confirming the formation of Ag NPs. After cooling it to room temperature, the formed Ag NPs were analyzed by UV-vis and FTIR spectroscopies, and their size was assessed by TEM and image analysis.

**3.3. Preparation of AgNP-WK/PVA solution.** 6 g WK powder was added to 50 mL water containing an appropriate quantity of NA-stabilized aqueous dispersion of Ag NP with slow stirring. The WK powder was then dissolved by adding concentrated sodium hydroxide solution drop-by-drop by maintaining the pH at no more than 9. After complete dissolution, the pH of the WK solution was almost neutral. A 10% aqueous solution of PVA was prepared by stirring and heating at 90 °C for 15 min and then the solution was cooled to 45°C with continuous stirring. 50 ml of 12% PVA solution was then added to AgNP-WK solution with stirring and both were homogeneously mixed. After removing the air bubbles, the solution was ready for electrospinning to form nanofibers on cotton fabric. The Ag NP content in the AgNP-WK/PVA solution was adjusted to 1 and 2% on the combined weight of WK and PVA. The fabric coated with a mixture of AgNP-WK and PVA solution without Ag NPs was used as a control.

**3.4. Electrospinning of AgNP-WK/PVA Nanofibrous Membrane onto Cotton Fabric.** The fabrication process of the nanofiber-deposited cotton wound dressing is presented by a schematic diagram in Figure 10, which is based on the schematic diagram of electrospinning of keratin/PVA published in our previous article.<sup>52</sup> The viscous 6% PVA, 1AgNP-WK-PVA, or 2AgNP-WK-PVA solution was loaded in a 10-mL size Terumo syringe, which was placed in a KDS syringe pump (Model 100, KDS Scientific, USA) to control the fluid flow fed to the spinneret. The electrospinning of AgNP-WK/PVA was conducted by using an Electrospinz electrospinning machine (Electrospinz Limited, Blenheim, New Zealand) at 20 kV DC power. A rotating stainless-steel drum of 5.5 cm diameter was used as a collecting screen. The rotating drum was covered with a cotton fabric sample and nanofibers were deposited on it. Electrospinning was performed at 20 °C and 45% relative humidity by maintaining a fixed needle-to-collector distance of 20 cm using a 1 mL/h<sup>1</sup> flow rate, which produced a nanofibrous membrane-coated cotton fabric sample. The mentioned conditions were found to be the best to produce bead-free uniform-sized nanofibers. Three types of samples were prepared, such as cotton fabric samples coated with WK/PVA, Ag NP-WK/PVA containing 0.1% Ag NPs, and Ag NP-WK/PVA containing 0.1% Ag NPs nanofibers. The electrospun nanofibrous membranes were crosslinked for 3 h by placing glutaraldehyde in a small Petri dish inside a round glass jar and placing the nanofiber-covered surface of the cotton fabric sample downward over the pen glass jar.

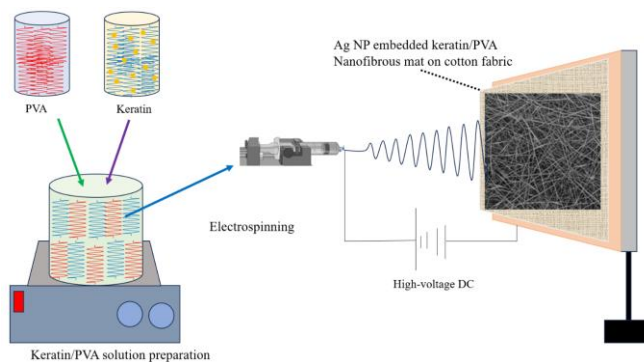


**Figure 10.** Schematic diagram of fabrication of AgNP-WK/PVA nanofibrous membrane on cotton fabric by electrospinning (modified from Ref 52 with copyright permission).

**3.5. Characterizations.** **3.4.1. Characterization of Ag NPs.** The UV-vis spectrum of NA-stabilized Ag NPs was acquired using an Evolution 220 UV-vis Spectrophotometer (Thermo Fisher Scientific Inc., Waltham, USA) at a wavelength interval of 1 nm in the 380–710 nm spectral span. TE. The Ag NP dispersion was concentrated by evaporating water and then a small amount of Ag NP dispersion was sprayed on a Formvar 200 mesh TEM copper grid, which was dried in a dust-free environment for 2 h. The Ag NP-coated copper grid was then scanned by using a Philips high-resolution TEM (Model: CM-200 FEG, Royal Philips Electronics,

Holland) and micrographs were captured by using a Gatan digital camera.

**3.4.2. SDS-PAGE Analysis.** To characterize the various proteins and their molecular weight distribution in the extracted keratin, sodium dodecyl sulfate-polyacrylamide gel electrophoresis (SDS-PAGE) was conducted. This method involves the initial denaturation of protein components with an anionic detergent (SDS), that also binds to them, imparting to all proteins a negative charge proportional to their molecular mass. Then electrophoresis through a porous acrylamide gel matrix is conducted to separate proteins with excellent resolution based on molecular mass. 7.5  $\mu\text{L}$  of protein sample (30  $\mu\text{g}$  of WK) was added to an appropriate volume of LDS sample loading buffer (4X) containing lithium dodecyl sulfate (Invitrogen Corporation, Waltham, USA) with 50 mM DTT and heated at 75  $^{\circ}\text{C}$  for 10 min to induce denaturation of the protein samples. The polyacrylamide gel colored with Coomassie Brilliant Blue R-250 dye was loaded in each run. The electrophoresis was conducted at room temperature at 80 V for 30 min and at 120 V for 60 min in 1X solution of NuPAGE MOPS SDS running buffer (Invitrogen) until the dye front reached the end of the 60 mm gel. A wide-range molecular weight (15–250 kDa) marker was run along with the proteins.

**3.4.3. Rheological Characterization of AgNP-WK/PVA Solutions.** The viscosity of the AgNP-WK/PVA solution was measured by using a LAMY viscometer (Model: RM100, LAMY Rheology Instruments, Champagne au Mont d'Or, France). The measurement time and temperature were 60 s and 22  $^{\circ}\text{C}$  respectively. To reach a valid overview of the behavior of the fluid, the viscosity was measured at shear rates between 0.96  $\text{s}^{-1}$  and 161  $\text{s}^{-1}$ .

**3.4.4. Characterization of AgNP-WK/PVA Nanofibrous Membrane.** A Thermo Scientific scanning electron microscope (Phenom Pure G6, Thermo Fisher Scientific Inc., Waltham, MA, USA) was used to study the morphology of the nanofibrous membrane. The recorded SEM photos were utilized to analyze the fiber diameter distribution behavior of the membrane, which was processed using ImageJ software (<https://imagej.nih.gov/ij/download.html>, accessed on 30 August 2023). The attenuated total reflectance-Fourier transform infrared (ATR-FTIR) spectra of 100% PVA and 50/50 AgNP-WK/PVA nanofibrous membranes were acquired with a Nicolet FTIR spectrophotometer (Model: Summit Pro, ThermoFisher Scientific Corporation, USA) using diamond crystal performing 128 scans with a resolution of 2  $\text{cm}^{-1}$  for each spectrum to achieve optimal signal-to-noise ratio. The contact angle of the untreated and treated wool fabrics was measured at 10 places on the coated surface by a KSV Contact Angle Measurement Apparatus (Model: CAM 100, KSV Instruments, Finland) and the average contact angle has been reported.

**3.6. Antibacterial Assessment.** The antibacterial properties of the untreated cotton fabric and cotton fabric coated with WK/PVA (WK-PVA) and AgNP-WK-PVA were measured according to the AATCC Test Method 147-1998 (*Assessment of Textile Materials: Parallel Streak Method*) against Gram-positive (*Staphylococcus aureus*) and Gram-negative (*Pseudomonas aeruginosa*) bacteria as they are

commonly available pathogens in wounds. 1 mL of 24 h broth culture of bacteria was diluted with 9 mL of sterile distilled water and one loopful of diluted inoculum was transferred to the surface of the sterile agar plate and 5 streaks of approximately 60 mm in length and spaced 10 mm apart covering the central area of a standard petri dish were made. The WK-PVA or AgNP-WK-PVA nanofiber-coated side of the fabrics (25 mm  $\times$  50 mm) were gently pressed transversely across the inoculum streaks to ensure intimate contact of nanofibrous membranes with the agar plate containing bacterial streak and incubated at 37  $\pm$  2  $^{\circ}\text{C}$  for 24 h. After this, the interruption of bacterial growth along the streaks of inoculum under the specimen and the zone of inhibition beyond its edge were examined. No growth of bacteria under the specimen indicates antibacterial activity, and the zone of inhibition indicates the leaching of antibacterial agent to the inoculum surrounding the test specimens. Usually for non-leaching type antibacterial agent-treated samples, no zone of bacterial inhibition is observed.

**3.7. In-vitro Cytocompatibility.** The MTT assay was conducted to determine the fibroblast cell viability against the prepared WK-PVA and AgNP-WK-PVA nanofibers. The fibroblast cells were cultured in a DMEM medium supplemented with 10% FBS and 1% penicillin/streptomycin antibiotic in an incubator at 37  $^{\circ}\text{C}$  under 5%  $\text{CO}_2$  for a specified time. Each experiment was conducted three times using a 96-well plate (3,000 cells/well) for the period of 1, 3, and 7 days as reported in published articles.<sup>53,54</sup> The absorbance of various samples was measured by a microplate reader (model: FLUOstar Omega, BMJ Labtech Corporation, USA) at 570 nm. Both sides of the WK-PVA and AgNP-WK-PVA nanofiber-deposited-cotton fabrics were sterilized under ultraviolet light for 30 min. Cells were seeded on WK-PVA and AgNP-WK-PVA nanofiber-deposited-cotton fabrics as well as control in 96-well plates at 3500 cells/well. Cell proliferation was investigated after 1, 3, and 7 days using CCK-8 assay. The optical density at 450 nm was recorded using the above-mentioned microplate reader. The calibration curve was prepared using the data obtained from the wells that contain known numbers of viable cells as shown in Figure S1 in Supporting Information.<sup>55</sup> A Student's t-test was conducted to compare the cytotoxicity data assuming unequal variances, considering a  $p < 0.01$  value.

**3.8. Assessment of release of Ag ions from cotton fabrics coated with AgNP-WK-PVA nanofibrous membrane.** The weight of the electrospun membrane deposited on a cotton fabric sample was measured by subtracting the weight of the cotton fabric. The actual amount of silver in the coated fabric was measured by dissolving the sample in 70% sulfuric acid followed by the addition of phosphate buffer solution to make a total 50 mL solution. The quantity of Ag was measured by the inductively coupled plasma-optical emission spectroscopy (ICP-OES) at RJ Hill Laboratories (Hamilton). For this purpose, we used a Thermo Scientific ICP-OES (Model: iCAP™ 7200 ICP-OES Analyzer Duo, Thermo Fisher Scientific Inc., Waltham, USA).

The release of Ag ions at various times from cotton fabric samples coated with AgNP-WK-PVA was measured after the

membrane-coated side of the cotton fabric samples was exposed to saturated vapor of glutaraldehyde, which caused cross-linking of PVA and keratin making the nanofibers insoluble in saline solution. An appropriate quantity of cotton fabric sample was submerged in 50 mL of PBS solution at pH ~7.4 and release of Ag ions was studied at 37 °C over 7 days. The Ag content of the solution was measured from time to time by the ICP-OES. Three samples were tested for each category and the averages are reported here.

#### 4. CONCLUSIONS

This work demonstrates that porous nanofibrous membranes of a 50/50 mixed solution of AgNP-WK and PVA can be deposited on cotton fabrics by electrospinning. The NA-reduced and stabilized Ag NPs were sphere-shaped with an average diameter of ~10 nm showing little agglomeration. The addition of AgNP-WK solution to PVA solution increased its viscosity due to the formation of hydrogen bonding between hydroxyl groups of PVA and amino and carboxyl groups of keratin. The electrospinning of 5% PVA solution formed nanofibers with a few beads but the 5% PVA + 5% AgNP-WK produced nanofibers without any visible bead formation, but the produced nanofibers had an increased diameter compared to the nanofibers made from 5% PVA solution. WK-PVA nanofibers deposited on cotton fabric showed no antibacterial activity, but cotton fabric coated with AgNP-WK-PVA showed excellent antibacterial activity and a reasonable level of cell viability for L-929 fibroblast cells. Nanofibrous membranes made from WK-PVA and AgNP-WK-PVA both had excellent hydrophilicity, which is good for the absorption of wound exudates. However, the increase in the Ag NP content negatively affected cell viability. The developed AgNP-WK-PVA nanofibers deposited on cotton show promising results as a wound dressing, which will pave the way for the development of new bioactive wound dressings. However additional research is needed to prove their wound healing properties by in-vivo testing on animals.

#### ASSOCIATED CONTENT

**Supporting Information.** The calibration curve was prepared using the data obtained from the wells that contain known numbers of viable cells, a figure showing the interaction between PVA and WK in the formation of WK-PVA nanofibers, and optical images of water droplets on uncoated and 1AgNP-keratin-PVA nanofiber coated cotton fabrics. This material is available free of charge via the Internet at <http://pubs.acs.org>.

#### AUTHOR INFORMATION

##### Corresponding Author

\* **Mohammad Mahbubul Hassan** – Bioproduct and Fiber technology team, Lincoln Research Center, AgResearch Limited, 1365 Springs Road, Lincoln 7674, Canterbury, New Zealand. Present address: Fashion Textiles and Technology Institute (FTTI), University of the Arts London, 105 Carpenter's Road, London E20 2AR, United Kingdom. <https://orcid.org/0000-0002-4120-6094>; E-mail: [mahbubul.hassan@arts.ac.uk](mailto:mahbubul.hassan@arts.ac.uk)

##### Authors

**Kira Heins** – Bioproduct and Fiber technology team, Lincoln Research Center, AgResearch Limited, 1365 Springs Road, Lincoln 7674, Canterbury, New Zealand. Present address: Institute of Textile Technology, RWTH Aachen University, Otto-Blumenthal-Str. 1, D-52074, Aachen, Germany.

**Haotian Zheng** – Department of Food, Bioprocessing, and Nutrition Sciences, North Carolina State University, Raleigh, NC 27695, USA.

##### Author Contributions

Conceptualization: M.M.H.; methodology: M.M.H.; validation: M.M.H.; formal analysis: M.M.H.; investigation: M.M.H, K.H., and H.Z.; resources: M.M.H and H.Z.; data curation: M.M.H. and K.H.; writing – original draft preparation: M.M.H. and K.H; writing – review and editing: M.M.H.; visualization: M.M.H and K.H.; supervision: M.M.H; project administration: M.M.H.; and funding acquisition: M.M.H. All authors have read and agreed to submit the manuscript.

##### Funding Sources

The funding for this work was provided by the Ministry of Business Innovation and Employment (MBIE) of the Government of New Zealand through Grant # C10X0824.

##### Notes

The authors declare no conflict of interest.

##### ACKNOWLEDGMENT

The authors acknowledge help received from Barbara Müller of R.J. Hills Limited for microbiological characterizations of various samples.

##### REFERENCES

- (1) Martinengo, L.; Olsson, M.; Bajpai, R.; Soljak, M.; Upton, Z.; Schmidtchen, A.; Car, J.; Järbrink, K. Prevalence of chronic wounds in the general population: systematic review and meta-analysis of observational studies. *Ann. Epidemiol.* **2019**, *29*, 8–15.
- (2) <https://www.who.int/news-room/fact-sheets/detail/ageing-andhealth#:~:text=At%20this%20time%20the%20share%2050%20to%20reach%20426%20million> (accessed on 27 October 2023).
- (3) Laurano, R.; Boffito, M.; Ciardelli, G.; Chiono, V. Wound dressing products: A translational investigation from the bench to the market, *Eng. Regen.* **3** (2022) 182–200.
- (4) Freedman, B. R.; Hwang, C.; Talbot, S.; Hibler, B.; Matoori, S.; Mooney, D. J. Breakthrough treatments for accelerated wound healing. *Sci. Adv.* **2023**, *9*, eade7007.
- (5) Byrd, A. L.; Belkaid, Y.; Segre, J. A. The human skin microbiome. *Nature Rev. Microbiol.* **2018**, *16*, 143–155.
- (6) Takeo, M.; Lee, W.; Ito, M. Wound healing and skin regeneration. *Cold Spring Harb. Perspect. Med.* **2015**, *5*, a023267.
- (7) Augustine, R.; Kalarikkal, N.; Thomas, S. Advancement of wound care from grafts to bioengineered smart skin substitutes. *Prog. Biomater.* **2014**, *3*, 103–113.
- (8) Guo, S.; DiPietro, L. A. Critical review in oral biology & medicine: Factors affecting wound healing. *J. Dental Res.* **2010**, *89*, 219–229.
- (9) DeLeon, S.; Clinton, A.; Fowler, H.; Everett, J.; Horswill, A. R.; Rumbaugh, K. P. Synergistic interactions of *Pseudomonas aeruginosa* and *Staphylococcus aureus* in an in vitro wound model. *Infect. Immun.* **2014**, *82*, 4718–4728.
- (10) Jenul, C.; Keim, K. C.; Jens, J. N.; Zeiler, M. J.; Schilcher, K.; Schurr, M. J.; Melander, C.; Phelan, V. V.; Horswill, A. R. Pyochelin

biotransformation by *Staphylococcus aureus* shapes bacterial competition with *Pseudomonas aeruginosa* in polymicrobial infections. *Cell Rep.* **2023**, *42*, 112540.

(11) Rivera, A. E.; Spencer, J. M. Clinical aspects of full-thickness wound healing. *Clin. Dermatol.* **2007**, *25*, 39–48.

(12) Strecker-McGraw, M. K.; Jones, T. R.; Baer, D. G. Soft tissue wounds and principles of healing. *Emerg. Med. Clin. N. Am.* **2007**, *25*, 1–22.

(13) Wu, X.; Liu, R.; Lao, T. T. Therapeutic compression materials and wound dressings for chronic venous insufficiency: A comprehensive review. *J. Biomed. Mater. Res. B Appl. Biomater.* **2020**, *108*, 892–909.

(14) Martin, L.; Wilson, C. G.; Koosha, F.; Tetley, L.; Gray, A. I.; Senel, S.; Uchegbu, I. F. The release of model macromolecules may be controlled by the hydrophobicity of palmitoyl glycol chitosan hydrogels. *J. Control Release* **2002**, *80*, 87–100.

(15) Thomas, A.; Harding, K. G.; Moore, K. Alginates from wound dressings activate human macrophages to secrete tumor necrosis factor- $\alpha$ . *Biomaterials* **2000**, *21*, 1797–802.

(16) Guillemain, Y.; Le Broc, D.; Sègalen, C.; Kurkdjian, E.; Guoze, J. N. Efficacy of a collagen-based dressing in an animal model of delayed wound healing. *J. Wound Care* **2016**, *25*, 406–413.

(17) Niiyama, H.; Kuroyanagi, Y. Development of novel wound dressing composed of hyaluronic acid and collagen sponge containing epidermal growth factor and vitamin C derivative. *J. Artif. Organs* **2014**, *17*, 81–87.

(18) Gomes Neto, R. J.; Genevro, G. M.; Paulo, L. D. A.; Lopes, P. S.; de Moraes, M. A.; Bepu, M. M. Characterization and in vitro evaluation of chitosan/konjac glucomannan bilayer film as a wound dressing. *Carbohydr. Polym.* **2019**, *212*, 59–66.

(19) Kim, D.; Kwon, S. -J.; Wu, X.; Sauve, J.; Lee, I.; Nam, J.; Kim, J.; Dordick, J. S. Selective killing of pathogenic bacteria by antimicrobial silver nanoparticle - Cell wall binding domain conjugates. *ACS Appl. Mater. Interf.* **2018**, *10*, 13317–13324.

(20) Murthy, M.B.; Krishnamurthy, B. Severe irritant contact dermatitis induced by povidone iodine solution. *Indian J. Pharmacol.* **2009**, *41*, 199–200.

(21) Wang, Y.; Li, P.; Xiang, P.; Lu, J.; Yuan, J.; Shen, J. Electrospun polyurethane/keratin/AgNP biocomposite mats for biocompatible and antibacterial wound dressings. *J. Mater. Chem. B* **2016**, *4*, 635–648.

(22) Singaravelu, S.; Ramanathan, G.; Muthukumar, T.; Raja, M. D.; Nagiah, N.; Thyagarajan, S.; Aravinthan, A.; Gunasekaran, P.; Natarajan, T. S.; Geetha Selva, G. V. N.; Kim, J. H.; Sivagnanam, U. T. Durable keratin-based bilayered electrospun mats for wound closure. *J. Mater. Chem. B* **2016**, *4*, 3982–3997.

(23) Konop, M.; Czuwara, J.; Kłodzińska, E.; Laskowska, A. K.; Zielenkiewicz, U.; Brzozowska, I.; Nabavi, S. M.; Rudnicka, L. Development of a novel keratin dressing which accelerates full-thickness skin wound healing in diabetic mice: In vitro and in vivo studies. *J. Biomater. Appl.* **2018**, *33*, 527–540.

(24) Ponrasu, T.; Veerasubramanian, P. K.; Kannan, R.; Gopika, S.; Suguna, L.; Muthuvijayan, V. Morin incorporated polysaccharide-protein (psyllium-keratin) hydrogel scaffolds accelerate diabetic wound healing in Wistar rats. *RSC Adv.* **2018**, *8*, 2305–2314.

(25) Giuri, D.; Barbalinardo, M.; Sotgiu, G.; Zamboni, R.; Nocchetti, M.; Donnadio, A.; Corticelli, F.; Valle, F.; Gennari, C. G. M.; Selmin, F.; Posati, T.; Aluigi, A. Nano-hybrid electrospun non-woven mats made of wool keratin and hydrocortisone as potential bioactive wound dressings. *Nanoscale* **2019**, *11*, 6422–6430.

(26) Yao, C. -H.; Lee, C. -Y.; Huang, C. -H.; Chen, Y. -S.; Chen, K. -Y. Novel bilayer wound dressing based on electrospun gelatin/keratin nanofibrous mats for skin wound repair. *Mater. Sci. Eng. C* **2017**, *79*, 533–540.

(27) Mirhaj, M.; Varshosaz, J.; Nasab, P.M.; Al-Musawi, M.H.; Almajidi, Y.Q.; Shahriari-Khalaji, M.; Tavakoli, M.; Alizadeh, M.; Sharifianjazi, F.; Mehrjoo, M.; Labbaf, S.; Sattar, M.; Esfahani, S.N. A

double-layer cellulose/pectin-soy protein isolate-pomegranate peel extract micro/nanofiber dressing for acceleration of wound healing. *Int. J. Biologic. Macromol.* **2024**, *255*, 128198.

(28) Tavakoli, M.; Mirhaj, M.; Varshosaz, J.; Al-Musawi, M.H.; Almajidi, Y.Q.; Danesh Pajooh, A.M.; Shahriari-Khalaji, M.; Sharifianjazi, F.; Alizadeh, M.; Labbaf, S.; Shahreabaki, K.E.; Nasab, P.M.; Firuzeh, M.; Esfahani, S.N. Keratin- and VEGF-incorporated honey-based sponge-nanofiber dressing: An ideal construct for wound healing. *ACS Appl. Mater. Interf.* **2023**, *15*, 55276–55286.

(29) Kavousi Heidari, M.; Pourmadadi, M.; Yazdian, F.; Rashedi, H.; Ebrahimi, S.A.S.; Bagher, Z.; Navaei-Nigjeh, M.; Haghirosadat, B.F. Wound dressing based on PVA nanofiber containing silk fibroin modified with GO/ZnO nanoparticles for superficial wound healing: In vitro and in vivo evaluations. *Biotechnol. Prog.* **2023**, *39*, e3331.

(30) Wang, X. -Y.; Mehadi Hassan, M.; He, X.; Hu, G.; Ren, Y.; Kim, H.; Mirkhani, S. A.; Hu, J.; Sen, A.; Wang, J.; Dong, T. G.; Lu, Q. Thymol-loaded polylactic acid electrospun fibrous membranes with synergistic biocidal and anti-bacterial adhesion properties via morphology control. *Colloid. Surf. A: Physicochem. Eng. Asp.* **2023**, *677*, 132360.

(31) Grizzo, A.; dos Santos, D. M.; da Costa, V. P. V.; Lopes, R. G.; Inada, N. M.; Correa, D. S.; Campana-Filho, S. P. Multifunctional bilayer membranes composed of poly(lactic acid), beta-chitin whiskers and silver nanoparticles for wound dressing applications. *Int. J. Biologic. Macromol.* **2023**, *251*, 126314.

(32) Mahmoudi, M.; Alizadeh, P.; Soltani, M. Wound healing performance of electrospun PVA/70S30C bioactive glass/Ag nanoparticles mats decorated with curcumin: In vitro and in vivo investigations. *Biomater. Adv.* **2023**, *153*, 213530.

(33) Jadidi Kouhbanani, M. A.; Mosleh-Shirazi, S.; Beheshtkhoo, N.; Kasaei, S. R.; Nekouian, S.; Alshehry, S.; Kamyab, H.; Chelliapan, S.; Ali, M. A.; Amani, A. M. Investigation through the antimicrobial activity of electrospun PCL nanofiber mats with green synthesized Ag-Fe nanoparticles. *J. Drug Deliv. Sci. Technol.* **2023**, *85*, 104541.

(34) Wang Y., Li P., Xiang P., Lu J., Yuan J., Shen J., Electrospun polyurethane/keratin/AgNP biocomposite mats for biocompatible and antibacterial wound dressings. *J. Mater. Chem. B* **2016**, *4*, 635–648.

(35) Sarviya, N.; Mahanta, U.; Dart, A.; Giri, J.; Deshpande, A. S.; Khandelwal, M.; Bhave, M.; Kingshott, P. Biocompatible and antimicrobial multilayer fibrous polymeric wound dressing with optimally embedded silver nanoparticles. *Appl. Surf. Sci.* **2023**, *612*, 155799.

(36) Sethuram, L.; Thomas, J.; Mukherjee, A.; Chandrasekaran, N. Eugenol micro-emulsion reinforced with silver nanocomposite electrospun mats for wound dressing strategies. *Mater. Adv.* **2021**, *2*, 2971–2988.

(37) Ider, M.; Abderrafi, K.; Eddahbi, A.; Ouaskit, S.; Kassiba, A. Silver Metallic Nanoparticles with Surface Plasmon Resonance: Synthesis and Characterizations. *J. Cluster Sci.* **2017**, *28*, 1051–1069.

(38) Chen, K.; Wang, F.; Liu, S.; Wu, X.; Xu, L.; Zhang, D. In situ reduction of silver nanoparticles by sodium alginate to obtain silver-loaded composite wound dressing with enhanced mechanical and antimicrobial property. *Int. J. Biologic. Macromol.* **2020**, *148*, 501–509.

(39) Suaroto, G.; Contardi, M.; Perotto, G.; Heredia-Guerrero, J. A.; Fiorentini, F.; Ceseracciu, L.; Pignatelli, C.; Debellis, D.; Bertorelli, R.; Athanassiou, A. From fabric to tissue: Recovered wool keratin/polyvinylpyrrolidone biocomposite fibers as artificial scaffold platform. *Mater. Sci. Eng. C* **2020**, *116*, 111151.

(40) Plowman, J. E.; Deb-Choudhury, S.; Thomas, A.; Clerens, S.; Cornillion, C. D.; Grosvenor, A. J.; Dyer, J. M. Characterization of low abundance wool proteins through novel differential extraction techniques. *Electrophoresis* **2010**, *31*, 1937–1946.

- (41) Varesano, A.; Aluigi, A.; Vineis, C.; Tonin, C. Study on the shear viscosity behavior of keratin/PEO blends for nanofiber electrospinning. *J. Polym. Sci. B Polym. Phys.* **2008**, *46*, 1193–1201.
- (42) Mansur, H. S.; Sadahira, C. M.; Souza, A. N. FTIR spectroscopy characterization of poly (vinyl alcohol) hydrogel with different hydrolysis degree and chemically crosslinked with glutaraldehyde. *Mater. Sci. Eng. C* **2008**, *28*, 539–548.
- (43) Refate, A.; Mohamed, Y.; Mohamed, M.; Sobhy, M.; Samhy, K.; Khaled, O.; Eidaroos, K.; Batikh, H.; El-Kashif, E.; El-Khatib, S.; Mehanny, S. Influence of electrospinning parameters on biopolymers nanofibers, with emphasis on cellulose & chitosan. *Heliyon* **2023**, *9*, e17051.
- (44) Hassan, M. M.; Leighs, S. J. Effect of surface treatments on physicochemical, stain-resist, and UV protection properties of wool fabrics. *Appl. Surf. Sci.* **2017**, *419*, 348–356.
- (45) Hassan, M. M. Wool fabrics coated with an anionic Bunte salt-terminated polyether: Physicochemical properties, stain resistance, and dyeability. *ACS Omega* **2018**, *3*, 17656–17667.
- (46) Tran, C. D.; Prosenyces, F.; Franko, M.; Benzi, G. Synthesis, structure and antimicrobial property of green composites from cellulose, wool, hair and chicken feather. *Carbohydr. Polym.* **2016**, *151*, 1269–1276.
- (47) Wang, X.; Mishra, B.; Lushnikova, T.; Narayana, J. L.; Wang, G. Amino acid composition determines peptide activity spectrum and hot-spot-based design of mercedin. *Adv. Biosys.* **2018**, *2*, 1700259.
- (48) Ji, H.; Zhou, S.; Fu, Y.; Wang, Y.; Mi, J.; Lu, T.; Wang, X.; Lü, C. Size-controllable preparation and antibacterial mechanism of thermo-responsive copolymer-stabilized silver nanoparticles with high antimicrobial activity. *Mater. Sci. Eng. C* **2020**, *110*, 110735.
- (49) Bragulla, H. H.; Homberger, D. G. Structure and functions of keratin proteins in simple, stratified, keratinized and cornified epithelia. *J. Anat.* **2009**, *214*, 516–559.
- (50) Archana, D.; Singh, B. K.; Dutta, J.; Dutta, P. K. Chitosan-PVP-nano silver oxide wound dressing: in vitro and in vivo evaluation. *Int. J. Biol. Macromol.* **2015**, *73*, 49–57.
- (51) Sarviya, N.; Mahanta, U.; Dart, A.; Giri, J.; Deshpande, A. S.; Khandelwal, M.; Bhave, M.; Kingshott, P. Biocompatible and antimicrobial multilayer fibrous polymeric wound dressing with optimally embedded silver nanoparticles. *Appl. Surf. Sci.* **2023**, *612*, 155799.
- (52) Pervez, M. N.; Hassan, M. M.; Naddeo, V. Separation of cationic methylene blue dye from its aqueous solution by S-sulfonated wool keratin-based sustainable electrospun nanofibrous membrane biosorbent. *Separat. Purification Technol.* **2024**, *333*, 125903.
- (53) Zafari, M.; Mansouri, M. B.; Omidghaemi, S.; Yazdani, A.; Pourmotabed, S.; Dehkordi, A. H.; Nosrati, H.; Validi, M.; Sharifi, E. Physical and biological properties of blend-electrospun polycaprolactone/chitosan-based wound dressings loaded with N-decyl-N, N-dimethyl-1-decanaminium chloride: an in vitro and in vivo study. *J. Biomed. Mater. Res. B Appl. Biomater.* **2020**, *108*, 3084–3098.
- (54) Nosrati, H.; Khodaei, M.; Banitalebi-Dehkordi, M.; Alizadeh, M.; Asadpour, S.; Sharifi, E.; Ai, J.; Soleimannejad, M. Preparation and characterization of poly(ethylene oxide)/zinc oxide nanofibrous scaffold for chronic wound healing applications. *Polim Med.* **2020**, *50*, 41–51.
- (55) Goodarzi, H.; Jadidi, K.; Pourmotabed, S.; Sharifi, E.; Aghamollaei, H. Preparation and in vitro characterization of cross-linked collagen-gelatin hydrogel using EDC/NHS for corneal tissue engineering applications. *Int. J. Biol. Macromol.* **2019**, *126*, 620–632.

SYNOPSIS TOC

A wound dressing based on Ag nanoparticle-embedded keratin/PVA nanofibers deposited on cotton fabric showed excellent antimicrobial activity, L-929 fibroblast cell viability, and cell proliferation.

